Earth and Planetary Science Letters 287 (2009) 329–332

Contents lists available at ScienceDirect

Earth and Planetary Science Letters

journal homepage: www.elsevier.com/locate/epsl

How does small-scale convection manifest in surface heat flux?

Jun Korenaga *

Department of Geology and Geophysics, Yale University, P.O. Box 208109, New Haven, CT 06520-8109, USA

A R T I C L E I N F O

Article history:
Received 12 March 2009
Received in revised form 10 July 2009
Accepted 11 August 2009
Available online 11 September 2009

Editor: Y. Ricard

Keywords:
mantle convection
heat flow
oceanic lithosphere

A B S T R A C T

Small-scale convection in the suboceanic mantle, if present, is commonly thought to manifest in surface heat flux, and the steady-state scaling of sublithospheric convection has often been used to interpret heat flow data from old ocean basins. Relations among small-scale convection, surface heat flux, and the steady-state scaling, however, have been vague. A series of transient cooling modeling are conducted here to quantify such relations. Given the strong temperature-dependency of mantle viscosity, results suggest that small-scale convection could take place without noticeably disturbing surface heat flux, and that the use of steady-state scaling may not be warranted for the present-day suboceanic mantle.

1. Introduction

The ocean floor represents the surface of the top boundary layer in mantle convection, and as the seafloor ages, the boundary layer (or oceanic lithosphere) gradually thickens by thermal diffusion (Turcotte and Schubert, 1982). The thickness of oceanic lithosphere may not increase indefinitely, however, because it could become dynamically unstable (Parsons and McKenzie, 1978; Davaille and Jaupart, 1994; Korenaga and Jordan, 2003). The existence of small-scale convection that prevents the growth of oceanic lithosphere has long been speculated from various kinds of observations including topography, heat flow, and seismic structure (e.g., Parsons and McKenzie, 1978; Lister et al., 1990; Montagner, 2002; Ritzwoller et al. 2004) and the focus of this article is on the relation between small-scale convection and heat flow.

Because small-scale convection modifies the thermal structure of lithosphere, its operation is expected to be reflected in surface heat flux. Earlier numerical and laboratory studies indicate that surface heat flux would divert considerably from that expected for simple half-space cooling, as soon as convection occurs (Davies, 1988; Davaille and Jaupart, 1994). A more recent analysis, however, suggests that the influence of small-scale convection on surface heat flux may be limited if the strong temperature-dependency of mantle viscosity is considered (Korenaga and Jordan, 2002), and one of the purposes of this paper is to quantify the effect of temperature-dependent viscosity on the timing of surface manifestation.

Also, small-scale convection has commonly been thought to achieve a quasi-steady-state shortly after its onset, and the scaling of stagnant-lid convection, which is valid for (statistically) steady state, has been used to interpret the heat flow data of old (>100 Ma) ocean basins (e.g., Davaille and Jaupart, 1994; Solomatov and Moresi, 2000). Even when small-scale convection is taking place, however, it is not obvious whether it should follow the steady-state scaling. A relation between transient cooling and steady-state scaling was previously investigated (Daly, 1980; Choblet and Sotin, 2000), but as explained later, it is yet to be understood when small-scale convection could achieve a quasi-steady-state in case of strongly temperature-dependent viscosity.

To address these timing issues, the transient cooling of a uniformly hot fluid is investigated for a range of Rayleigh numbers and the temperature-dependency of viscosity. A model setup will be explained next, followed by numerical results. The implications for the dynamics of suboceanic mantle will be discussed briefly at the end.

2. Model formulation and results

Numerical formulation follows closely that of Korenaga and Jordan (2003); a uniformly hot fluid with temperature-dependent viscosity is subject to instantaneous cooling and no internal heating at $t^*=0$ (asterisk indicates a nondimensionalized variable and time is normalized by the diffusion time scale of D^2/κ, where D is the system depth and κ is thermal diffusivity). The nondimensionalized governing equations for thermal convection in an incompressible fluid are solved by the 2-D finite element code of Korenaga and Jordan (2003). The top and bottom boundaries are free slip. Temperature is normalized by ΔT, which is the difference between the surface temperature and the initial internal temperature. The top temperature is fixed to 0, and the bottom boundary is insulating. A reflecting boundary condition (i.e., free slip and insulating) is applied to the side boundaries. Internal temperature is set to 1 at $t^*=0$. The aspect ratio

* Tel.: +1 203 432 7381; fax: +1 203 432 3134.
E-mail address: jun.korenaga@yale.edu.

0012-821X/$ – see front matter © 2009 Elsevier B.V. All rights reserved.
doi:10.1016/j.epsl.2009.08.015

of a model is four to eliminate wall effects, and the model is discretized by 256×64 uniform quadrilateral elements. The amplitude of random perturbation in the initial temperature field is 10^{-5}, and the following linear–exponential viscosity is employed:

$$\mu^*(T^*) = exp[\theta(1 - T^*)], \tag{1}$$

where θ is the Frank–Kamenetskii parameter. Viscosity is normalized by reference viscosity μ_0, which corresponds to viscosity at $T^* = 1$.

The convection system is characterized by two nondimensional parameters, the above Frank–Kamenetskii parameter and the Rayleigh number defined as

$$Ra = \frac{\alpha \rho_0 g \Delta T D^3}{\kappa \mu_0}, \tag{2}$$

where α is thermal expansivity and ρ_0 is reference density. All combinations of five Rayleigh numbers (10^7, 3×10^7, 10^8, 3×10^8, and 10^9), and five Frank–Kamenetskii parameters (9, 12, 15, 18, and 21) are considered. An 'effective' activation energy for the temperature-dependency of upper mantle viscosity is likely to be ~300 kJ mol^{-1} regardless of creep mechanisms (Korenaga, 2006; Korenaga and Karato, 2008), which is equivalent to θ of ~18.5 (assuming the temperature scale of 1350 K). As far as the physics of small-scale convection is concerned, it is immaterial whether linear–exponential or Arrhenius viscosity is used. Both types of temperature-dependent viscosity result in similar dynamics (Reese et al., 1999; Korenaga and Jordan, 2003). My choice here is to facilitate direct comparison with the scaling law of stagnant-lid convection (Solomatov and Moresi, 2000), which is built on numerical simulation with linear–exponential viscosity.

Numerical modeling here is limited to 2-D, but it is sufficient to capture relevant physics for the following reasons. First, whether 2-D or 3-D does not matter for the onset of convection in a horizontally infinite layer (Chandrasekhar, 1981). More critical is the restriction of modes by wall effects (Davis, 1967; Korenaga and Jordan, 2001), which should be minimized by the use of the large aspect ratio. Three-dimensionality becomes important for finite-amplitude convection, in particular regarding its spatial configuration. The planform of small-scale convection beneath oceanic plate has long been thought to be influenced by vertical shear associated with plate motion (e.g., Richter, 1973). To minimize the interference with such background flow, convection cells tend to align in parallel to plate motion, and the dynamics of small-scale convection becomes 2-D, being decoupled from vertical shear (Jeffreys, 1928; Ingersoll, 1966; Richter and Parsons, 1975). The temporal evolution of sublithospheric convection can thus be well captured by 2-D models if such models are interpreted as the cross section of suboceanic mantle perpendicular to plate motion (e.g., Buck and Parmentier, 1986; Korenaga and Jordan, 2004). Finally, the scaling law of stagnant-lid convection adopted here is also built on 2-D models (Solomatov and Moresi, 2000). More important, the scaling of stagnant-lid convection can be derived by the local stability analysis of thermal boundary layer (Solomatov, 1995), indicating that 2-D treatment is sufficient as for the onset of convection.

The onset time of convection, t_c^*, is defined as the time when the kinetic energy of the system exceeds its initial value by more than three orders of magnitude (Fig. 1a and b). After the onset, the surface heat flux, q^*, starts to deviate from what is expected for half-space cooling (i.e., $1/\sqrt{\pi t^*}$), and the time when the deviation exceeds 5% of the half-space prediction is marked as t_5^*. The internal temperature, T_i^*, is calculated by averaging the temperature field beneath the thermal boundary layer (Fig. 1c). Steady-state heat flux, q_s^*, is then calculated from the following scaling law for stagnant-lid convection (Solomatov and Moresi, 2000):

$$q_s^*\left[1-2\left(1-2.4\theta_i^{-1}\right)/q_s^*\right]^{1/2} = 0.53\theta_i^{-4/3}Ra_i^{1/3}, \tag{3}$$

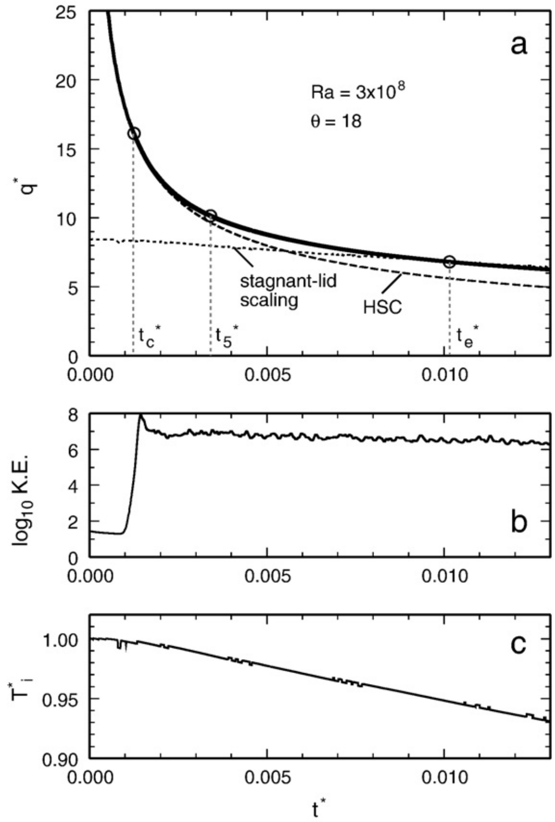

Fig. 1. Example of numerical solutions in case of Ra of 3×10^8 and θ of 18. (a) Surface heat flux as a function of diffusion time t^*. Numerical solution (solid) is compared with the half-space cooling prediction (dashed) and the stagnant-lid scaling (dotted). (b) Kinetic energy. (c) Internal temperature.

where Ra_i and θ_i are redefined Rayleigh number and Frank–Kamenetskii parameter, respectively, as $Ra_i = Ra\ \exp[-\theta(1-T_i^*)]$ and $\theta_i = \theta T_i^*$. The time when surface heat flux matches the steady-state prediction is denoted as t_e^* (Fig. 1a).

The use of the term 'steady-state' here may require some clarification because it does not refer to time-independent convection. When the Rayleigh number is sufficiently high, convection is usually chaotic and highly time-dependent, but it is still possible to define a statistically steady state at which time-averaged quantities converge. The scaling law of Eq. (3) is based on such steady-state solutions. This steady-state heat flux is a function of Ra_i and θ_i, both of which depend on the internal temperature T_i^*. Because T_i^* slowly decreases in a system cooled from above (Fig. 1c), heat flow predicted by the steady-state scaling also changes with time (Fig. 1a). Thus, it should be understood as the amount of heat flow expected when small-scale convection is in a statistically steady state with given Ra_i and θ_i.

As Fig. 2a shows, the ratio t_5^*/t_c^* increases almost linearly as θ increases, and for θ~20, it takes three times longer to have a noticeable heat flow anomaly than just to have the onset of convection. This tendency of delayed surface manifestation may already be recognized in Fig. 2 of Korenaga and Jordan (2002), but Fig. 2a here demonstrates that there is a simple linear relation independent of the Rayleigh number. The scaling law for the onset of convection (Korenaga and Jordan, 2003) suggests that the onset times for different model runs should collapse onto a single curve if they are normalized by the local boundary layer time scale t_r^* of $Ra^{-2/3}$, which is indeed the case (Fig. 2b). Similar data collapse is also achieved for the equilibration time t_e^*, but data are more scattered for greater θ because the steady-state prediction and the measured heat flux tend to cross at smaller angles. As for t_5^*, t_e^*/t_c^* increases for larger θ. This behavior may be

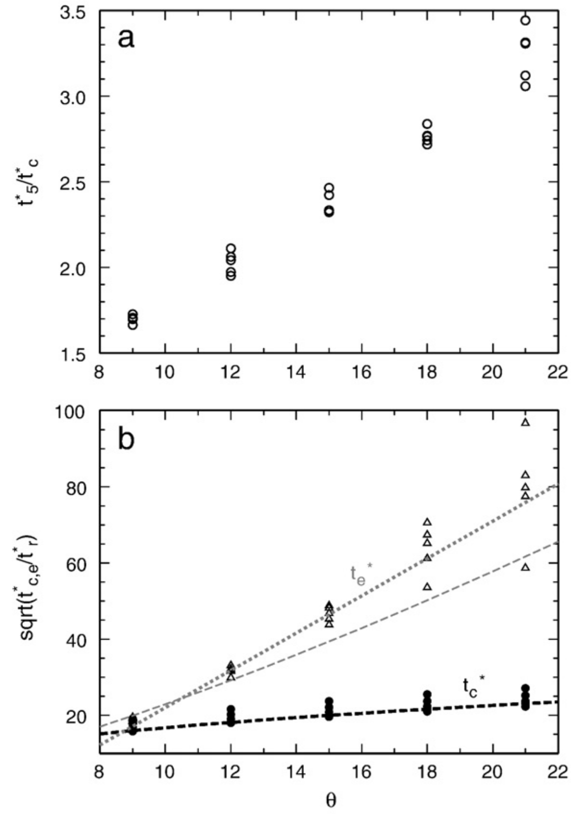

Fig. 2. Summary of timing measurements. (a) t_5^*/t_c^* as a function of θ. (b) The square root of onset time t_c^* and equilibration time t_e^* scaled by local boundary layer timescale t_r^* as a function of θ. The scaling law of onset time (Korenaga and Jordan, 2003) with the critical Rayleigh number of 2×10^3 is shown by solid dashed. Gray dashed corresponds to the scaling of Eq. (5), and gray dotted ($-27+4.9\,\theta$) is a fit to the trend of $\sqrt{t_e^*/t_r^*}$.

understood as follows. At $t^*=t_e^*$, surface heat flux is equal to a prediction from the scaling of stagnant-lid convection, i.e.,

$$\frac{1}{\sqrt{\pi t_e^*}}\approx 0.53\theta^{-4/3}Ra^{1/3}, \tag{4}$$

where I use half-space cooling to approximate surface heat flux and neglect variations in θ and Ra due to the temporal evolution of T_i. Note that the asymptotic limit of Eq. (3) is used here. This relation should place a lower bound on t_e^*, because the left-hand side is a lower bound for actual surface heat flux and the right-hand side is an approximate upper bound for stagnant-lid prediction (Fig. 1). Eq. (4) may be rearranged as

$$\sqrt{t_e^*/t_r^*}\approx\frac{\theta^{4/3}}{0.53\sqrt{\pi}}. \tag{5}$$

As shown in Fig. 2b, this scaling indeed serves approximately as a lower bound; the actual measurements of $\sqrt{t_e^*/t_r^*}$ may be better represented by a linear fit of $-27+4.9\theta$, which will be used in subsequent discussion.

3. Discussion and conclusion

Scaling for the thermal adjustment time scale, in case of convection with temperature-dependent viscosity, was previously studied by Choblet and Sotin (2000), who derived the following:

$$\Delta t^*=t_e^*-t_c^*\approx 0.73\delta^2, \tag{6}$$

where δ is the lid thickness at $t^*=t_e^*$. Because the lid thickness grows approximately as $\sqrt{t^*}$, the above scaling is equivalent to

$$t_e^*-t_c^*\approx t_e^*, \tag{7}$$

which implies that $t_c^*\ll t_e^*$. Eq. (7) is also supported by the data obtained in this study, and t_c^*/t_e^* is indeed much less than unity for most cases (Fig. 3). This means that Eq. (6) is essentially the identity equation of $t_e^*=t_e^*$. One cannot derive the θ-dependence of t_e^* (Fig. 2b) from the scaling of Choblet and Sotin (2000).

A dimensionalized example is given in Fig. 4, for which the following properties are used: thermal expansivity of 2×10^{-5} K^{-1}, density of 4000 kg m^3, gravitational acceleration of 9.8 m s^{-2}, temperature contrast of 1350 K, thermal diffusivity of 10^{-6} m^2 s, and activation energy of 300 kJ mol^{-1}. Asthenospheric viscosity (viscosity at $T^*=1$) is varied from 10^{17} Pa s to 10^{20} Pa s. The present-day asthenospheric viscosity may be ~10^{19} Pa s (e.g., Hager, 1991), and lower viscosity would correspond to the situation in the geological past when the mantle was hotter. Though the estimate of asthenospheric viscosity has been controversial, ranging from ~10^{18} Pa s to ~10^{20} Pa s (e.g., Hager, 1991; Davaille and Jaupart, 1994; Watts and Zhong, 2000), the seismic structure of the upper mantle beneath the Pacific implies that small-scale convection may start to take place beneath ~50–70 Ma seafloor (e.g., Montagner, 2002; Ritzwoller et al., 2004), corresponding to the viscosity of ~10^{19} Pa s (Fig. 4). Because t_5^*/t_c^* is ~3 for the given θ, noticeable heat flow anomalies (>5%) would appear only when the seafloor becomes older than ~150 Ma. The oldest seafloor at the present day is ~180 Ma (Muller et al., 1997), so the bulk of surface heat flow is expected to be explained well by simple half-space cooling, which may actually be the case (Korenaga and Korenaga, 2008). In other words, the absence of notable deviation from half-space cooling does not necessarily contradict the operation of small-scale convection under the most of ocean basins (older than

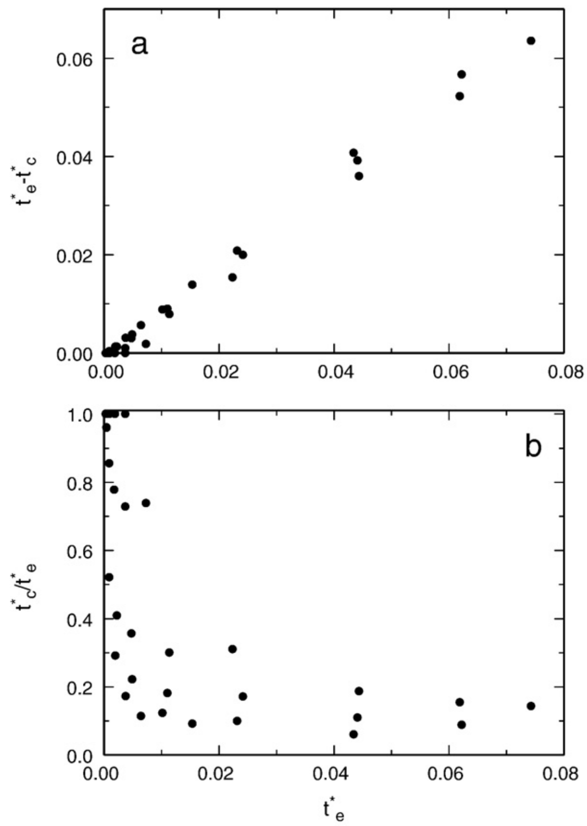

Fig. 3. On the scaling of thermal adjustment timescale. (a) t_e^*/t_c^* and (b) t_c^*/t_e^* are plotted as a function of t_e^*. See text for discussion.

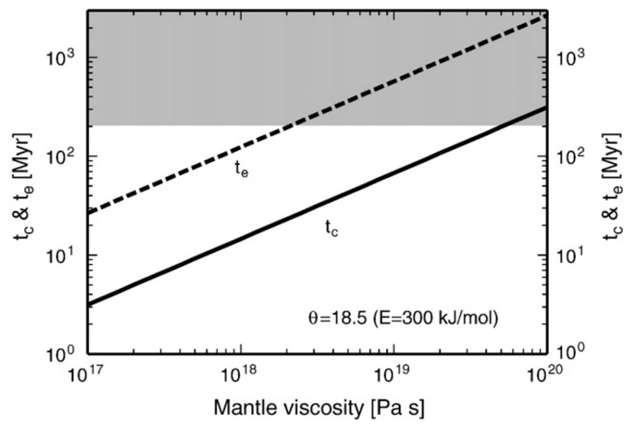

Fig. 4. Onset time of convection (t_c, solid) and equilibration time (t_e, dashed) as a function of (asthenospheric) mantle viscosity. The activation energy is assumed to be 300 kJ mol^{-1}. Gray shading ($t > 200$ Myr) signifies the region unobservable in the present-day seafloor.

~50 Ma). This study by itself does not disprove the possibility of elevated heat flow in old ocean basins; if convection takes place beneath 30 Ma seafloor, for example, more than 5% deviation in heat flow is expected for >90 Ma. An important point is that there is a considerable time lag between the onset of convection and its manifestation in surface heat flow.

The equilibration time t_e is ~8 ± 2 times greater than t_c (Fig. 2b), and when mantle viscosity is lower than 10^{18} Pa s, t_e is smaller than ~100 Myr. The use of the steady-state scaling of stagnant-lid convection could be justified when modeling the thermal history of terrestrial planets such as Venus and Mars (e.g., Solomatov and Moresi, 1996; Reese et al.1998) because a hotter mantle in the past probably had low viscosity. A similar conclusion was arrived previously (Choblet and Sotin, 2000); the only major difference would be the derivation of the correct scaling (Eq. (5); Fig. 2), which is essential to judge whether the steady-state scaling is applicable at regional scales such as small-scale convection beneath oceanic lithosphere. If the onset of convection takes place at ~50 Myr, t_e could be as long as ~400 ± 100 My at the present-day condition, so steady-state convection may not be achieved in the suboceanic mantle. These findings suggest that it is more challenging than usually thought to infer subsurface processes from surface heat flow. But knowing the strength of heat flow data with respect to other observational constraints would be important when synthesizing them to approach the true dynamic state of suboceanic mantle.

Acknowledgments

The author thanks Editor Yanick Ricard, Joerg Schmalzl, and two anonymous reviewers for constructive comments. This work was sponsored by the U.S. National Science Foundation under Grant EAR-0449517.

References

Buck, W.R., Parmentier, E.M., 1986. Convection beneath young oceanic lithosphere: implications for thermal structure and gravity. J. Geophys. Res. 91, 1961–1974.

Chandrasekhar, S., 1981. Hydrodynamic and Hydromagnetic Stability. Dover, New York.

Choblet, G., Sotin, C., 2000. 3D thermal convection with variable viscosity: can transient cooling be described by a quasi-static scaling law? Phys. Earth Planet. Int. 119, 321–336.

Daly, S.F., 1980. Convection with decaying heat sources: constant viscosity. Geophys. J. R. Astron. Soc. 61, 519–547.

Davaille, A., Jaupart, C., 1994. Onset of thermal convection in fluids with temperature-dependent viscosity: application to the oceanic mantle. J. Geophys. Res. 99, 19853–19866.

Davies, G.F., 1988. Ocean bathymetry and mantle convection: 2. small-scale flow. J. Geophys. Res. 93, 10481–10488.

Davis, S.H., 1967. Convection in a box: linear theory. J. Fluid Mech. 30, 465–478.

Hager, B.H., 1991. Mantle viscosity: a comparison of models from postglacial rebound and from the geoid, plate driving forces, and advected heat flux. In: Sabadini, R., Lambeck, K., Boschi, E. (Eds.), Glacial Isostasy, Sea-Level and Mantle Rheology. Kluwer Academic, Dordrecht, pp. 493–513.

Ingersoll, A.P., 1966. Thermal convection with shear at high Rayleigh number. J. Fluid Mech. 25, 209–228.

Jeffreys, H., 1928. Some cases of instability in fluid motion. Proc. R. Soc. Lond. A 118, 195–208.

Korenaga, J., 2006. Archean geodynamics and the thermal evolution of Earth. In: Benn, K., Mareschal, J.-C., Condie, K. (Eds.), Archean Geodynamics and Environments. American Geophysical Union, Washington, D.C., pp. 7–32.

Korenaga, J., Jordan, T.H., 2001. Effects of vertical boundaries on infinite Prandtl number thermal convection. Geophys. J. Int. 147, 639–659.

Korenaga, J., Jordan, T.H., 2002. On 'steady-state' heat flow and the rheology of oceanic mantle. Geophys. Res. Lett. 29 (22), 2056. doi:10.1029/2002GL016085.

Korenaga, J., Jordan, T.H., 2003. Physics of multiscale convection in Earth's mantle: onset of sublithospheric convection. J. Geophys. Res. 108 (B7), 2333. doi:10.1029/2002JB001760.

Korenaga, J., Jordan, T.H., 2004. Physics of multiscale convection in Earth's mantle: evolution of sublithospheric convection. J. Geophys. Res. 109, B01405. doi:10.1029/2003JB002464.

Korenaga, J., Karato, S., 2008. A new analysis of experimental data on olivine rheology. J. Geophys. Res. 113, B02403. doi:10.1029/2007JB005100.

Korenaga, T., Korenaga, J., 2008. Subsidence of normal oceanic lithosphere, apparent thermal expansivity, and seafloor flattening. Earth Planet. Sci. Lett. 268, 41–51.

Lister, C.R.B., Sclater, J.G., Davis, E.E., Villinger, H., Nagihara, S., 1990. Heat flow maintained in ocean basins of great age: investigations in the north-equatorial west Pacific. Geophys. J. Int. 102, 603–628.

Montagner, J., 2002. Upper mantle low anisotropy channels below the Pacific plate. Earth Planet. Sci. Lett. 202, 263–374.

Muller, R.D., Roest, W.R., Royer, J.-Y., Gahagan, L.M., Sclater, J.G., 1997. Digital isochrons of the world's ocean floor. J. Geophys. Res. 102, 3211–3214.

Parsons, B., McKenzie, D., 1978. Mantle convection and the thermal structure of the plates. J. Geophys. Res. 83, 4485–4496.

Reese, C.C., Solomatov, V.S., Moresi, L.-N., 1998. Heat transport efficiency for stagnant lid convection with dislocation viscosity: application to Mars and Venus. J. Geophys. Res. 103 (E6), 13643–13657.

Reese, C.C., Solomatov, V.S., Moresi, L.-N., 1999. Non-Newtonian stagnant lid convection and magmatic resurfacing on Venus. Icarus 139, 67–80.

Richter, F.M., 1973. Convection and the large-scale circulation of the mantle. J. Geophys. Res. 78, 8735–8745.

Richter, F.M., Parsons, B., 1975. On the interaction of two scales of convection in the mantle. J. Geophys. Res. 80, 2529–2541.

Ritzwoller, M.H., Shapiro, N.M., Zhong, S., 2004. Cooling history of the Pacific lithosphere. Earth Planet. Sci. Lett. 226, 69–84.

Solomatov, V.S., 1995. Scaling of temperature- and stress-dependent viscosity convection. Phys. Fluids 7, 266–274.

Solomatov, V.S., Moresi, L.-N., 1996. Stagnant lid convection on Venus. J. Geophys. Res. 101 (E2), 4737–4753.

Solomatov, V.S., Moresi, L.-N., 2000. Scaling of time-dependent stagnant lid convection: application to small-scale convection on earth and other terrestrial planets. J. Geophys. Res. 105, 21795–21817.

Turcotte, D.L., Schubert, G., 1982. Geodynamics: Applications of Continuum Physics to Geological Problems. John Wiley, New York.

Watts, A.B., Zhong, S., 2000. Observations of flexure and the rheology of oceanic lithosphere. Geophys. J. Int. 142, 855–875.